

Computing Bounds for Linear Functionals of Exact Weak Solutions to Poisson's Equation

A. M. Sauer-Budge¹, A. Huerta², J. Bonet³ and J. Peraire¹

¹Department of Aeronautics and Astronautics, Massachusetts Institute of Technology, USA

²Departamento de Matematica Aplicada III, Universitat Politecnica de Catalunya, Spain

³Department of Civil Engineering, University of Wales Swansea, UK

Abstract— We present a method for Poisson's equation that computes guaranteed upper and lower bounds for the values of linear functional outputs of the exact weak solution of the infinite dimensional continuum problem using traditional finite element approximations. The guarantee holds uniformly for any level of refinement, not just in the asymptotic limit of refinement. Given a finite element solution and its output adjoint solution, the method can be used to provide a certificate of precision for the output with an asymptotic complexity which is linear in the number of elements in the finite element discretization.

Keywords— Finite Element, Output Bounds, A Posteriori Error Estimation, Poisson Equation

I. INTRODUCTION

UNCERTAINTY about the reliability of numerical approximations frequently undermines the utility of field simulations in the engineering design process: simulations are often not trusted or are more costly than necessary. In addition to devitalized confidence, numerical uncertainty often causes ambiguity about the source of any discrepancies when using simulation results in concert with experimental measurements. Can the discretization error account for the discrepancies, or is the underlying continuum model inadequate? To disambiguate, we define *precision* to be the ability to increase the fidelity of simulation, through decreasing the mesh diameter or increasing the approximation order, and obtain consistent results for a given number of significant digits, and we define *accuracy* to be the conformity of a simulation result to physical fact.

While confidence in the precision of a field simulation can be bolstered by performing convergence studies, such studies are computationally very expensive and in practice are often not performed at more than a few conditions, if at all, due to cost and time constraints. For this reason, researchers and practitioners employ adaptive methods to converge the solution in a manner which costs less in time and resources than uniform refinement. Adaptive methods powered by current error estimation technology, however, provide only asymptotic guarantees of precision, at best, and no guarantees of precision, at worse, since the convergence of adaptive methods remains an open question [1]. Moreover, asymptotic estimates only ensure the precision of well-refined results with relatively many significant digits, while only relatively few significant digits may be desired.

Our observations of engineering practice inform us that integrated quantities such as forces and total fluxes are

frequently queried quantitative outputs from field simulations and that design and analysis does not always require the full precision available. The primary objective of our method, therefore, is to certify the precision of integrated outputs for the available range of significant digits— for low fidelity simulations as well as high fidelity simulations. We call our bounds *uniform* to differentiate our goal of obtaining quantitative bounds for all levels of refinement from the lesser goal of obtaining quantitative bounds only asymptotically in the limit of refinement.

Verification and *a posteriori* error analysis have a long history in the development of the finite element method with many different approaches forwarded and investigated. Ainsworth gives a detailed overview of many of the approaches in [2]. Conceptually, our method descends from a long line of complementary energy methods beginning in the early 1970s when Fraeijs de Veubeke [3] proposed verifying the precision of a simulation by comparing the energy computed from a global primal approximation with the complementary energy computed from a global dual approximation. Global primal-dual methods offer a rich context for approximation, but suffer from the delicate nature of the global dual approximation, relatively high cost, particularly for nonlinear problems, and for verification, from a lack of relevant measure, because the upper and lower bounding properties only hold for the total energy.

Much more closely related to our work are the works of Ladevèze [4], Kelly [5] and of Destuynder [6], all of which consider local complementary energy problems for developing estimates for the energy norm of the error. In contrast to the work of Ladevèze, we endeavor to compute guaranteed two-sided bounds on outputs, not an estimate of the error in an abstract norm. Our method differs from that of Kelly in that we obtain bounds for general meshes and more general boundary conditions, and from that Destuynder in that our method is not burdened with the construction of a globally dual admissible field. The work we present here descends directly from earlier work done by Paraschivoiu, Peraire and Patera [7], [8] on two-level residual based techniques for computing output bounds.

A. Poisson's Equation

We consider Poisson's equation posed on polygonal domains, Ω , and, only for the sake of simplicity of presentation, all homogeneous Dirichlet boundaries, $\Gamma = \partial\Omega$. The Poisson problem is formulated weakly as: find $u \in \mathcal{U}$ such

that

$$\int_{\Omega} \nabla u \cdot \nabla v \, d\Omega = \int_{\Omega} f v \, d\Omega, \quad \forall v \in \mathcal{U}, \quad (1)$$

where $\mathcal{U}(\Omega) \equiv \{u \in \mathcal{H}^1(\Omega) \mid u|_{\Gamma \cap \partial\Omega} = 0\}$ and the domain Ω is assumed when otherwise unspecified, that is, $\mathcal{U} \equiv \mathcal{U}(\Omega)$. As a consequence of all the Dirichlet boundaries being homogeneous, \mathcal{U} serves as both the function set and test space in our presentation. While we present the method for homogeneous Dirichlet data, it can be easily extended to non-homogeneous data, and Neumann boundary conditions.

II. ENERGY BOUNDS

We begin by developing a lower bound on the total energy¹ of the system, $\frac{1}{2} \int_{\Omega} \nabla u \cdot \nabla u \, d\Omega - \int_{\Omega} f u \, d\Omega$, which in the context of heat conduction, combines the heat dissipation energy, $\frac{1}{2} \int_{\Omega} \nabla u \cdot \nabla u \, d\Omega$, and the potential energy of the thermal loads, $-\int_{\Omega} f u \, d\Omega$. There is a well known physical principle at work in this problem, related to the symmetric positive definite nature of the diffusion operator, which states that the solution, u , is the function which minimizes the total energy with respect to all other candidates in \mathcal{U}

$$u = \arg \inf_{w \in \mathcal{U}} \frac{1}{2} \int_{\Omega} \nabla w \cdot \nabla w \, d\Omega - \int_{\Omega} f w \, d\Omega, \quad (2)$$

as can easily be verified by comparing the Euler-Lagrange equation of this minimization statement to Poisson's equation (1). This minimization formulation makes it clear that if we look for a discrete approximation of Poisson's equation (1) in a finite set of conforming functions, \mathcal{U}_h , for which $\mathcal{U}_h \subset \mathcal{U}$, then the resulting total energy predicted by the approximation will approach the exact value from above.

While insightful, this upper bound on the total energy has limited usefulness for two primary reasons. First, only rarely will the total energy be relevant to the purpose of the solving the original problem. Second, even when it is relevant, the upper bound will most likely not be helpful for managing approximation uncertainty. In an engineering design task, the upper bound usually corresponds to the "best case scenario," as opposed to the "worst case scenario" which would be required to ensure feasibility of the design.

Our strategy for obtaining lower bounds on the energy is to first relax the continuity of the set \mathcal{U} along edges of the partitioning of Ω induced by the finite element approximation using approximate Lagrange multipliers computed from the finite element approximation of Poisson's equation (1), then build-up the lower bound subdomain-by-subdomain by finding feasible solutions to a local dual problem and computing its objective value, the well-known complementary energy.

A. Weak Continuity

A finite element discretization of Poisson's equation (1) will partition the domain into a mesh, \mathcal{T}_h , of non-

¹The energy is commonly defined to be $\frac{1}{2} \int_{\Omega} \nabla u \cdot \nabla u \, d\Omega$ which considering (1) is the negative of what we have defined to be the energy.

overlapping open sub-domains, T , called elements, for which $\bigcup_{T \in \mathcal{T}_h} \bar{T} = \bar{\Omega}$. We denote by ∂T the edges constituting the boundary of a single element T , and by $\partial \mathcal{T}_h$ the network of all edges in the mesh. We have not yet evoked the discretization of \mathcal{U} associated with the finite element method, but merely the domain decomposition introduced by the mesh. With the broken space

$$\hat{\mathcal{U}} \equiv \{v \mid v \in L^2(\Omega), v|_T \in \mathcal{H}^1(T), \forall T \in \mathcal{T}_h\}, \quad (3)$$

in which the continuity of \mathcal{U} is broken across the mesh edges, $\partial \mathcal{T}_h$, we can re-formulate the energy minimization statement (2) by explicitly enforcing continuity

$$\begin{aligned} \inf_{\hat{w} \in \hat{\mathcal{U}}} & \frac{1}{2} \int_{\Omega} \nabla \hat{w} \cdot \nabla \hat{w} \, d\Omega - \int_{\Omega} f \hat{w} \, d\Omega \\ \text{s.t.} & \sum_{T \in \mathcal{T}_h} \int_{\partial T} \sigma_T \lambda \hat{w} \, d\Gamma = 0, \quad \forall \lambda \in \Lambda, \end{aligned} \quad (4)$$

where, for $T_N \in \mathcal{T}_h$ and an arbitrary ordering of the elements, $T < T_N$,

$$\sigma_T(x) = \begin{cases} -1 & x \in \bar{T} \cap \bar{T}_N, T < T_N \\ +1 & \text{otherwise.} \end{cases} \quad (5)$$

Since \hat{w} is a member of $\mathcal{H}^1(T)$, the trace of \hat{w} on γ is a member of $\mathcal{H}^{1/2}(\partial T)$ and λ is a member of the dual of the trace space, $\Lambda(\partial T) = \mathcal{H}^{-1/2}(\partial T)$. As there is no ambiguity, we have suppressed the trace operators from our notation for the boundary integrals to simplify the appearance of the expressions.

Notice that we have relaxed the Dirichlet boundary conditions as well as the interior continuity. The homogeneous Dirichlet conditions are weakly enforced implicitly by the continuity constraint. We shall not prove it here, but it is important to note that the minimizer of this constrained minimization problem is indeed u , the exact solution of Poisson's equation (1).

To see how this constraint arises, consider a single edge, $\gamma \in \partial \mathcal{T}_h$, with neighboring elements T and T_N , for which a strong continuity constraint can be written roughly as $\hat{w}|_{T,\gamma} - \hat{w}|_{T_N,\gamma} = 0$ on γ . A Galerkin-weak representation is obtained by multiplying by an arbitrary test function, λ_γ , taken from an appropriate space, $\Lambda(\gamma)$, integrating along the edge, and ensuring the resulting integrated quantity is zero for all possible test functions: $\int_{\gamma} (\hat{w}|_{T,\gamma} - \hat{w}|_{T_N,\gamma}) \lambda_\gamma \, d\Gamma = 0, \quad \forall \lambda_\gamma \in \Lambda(\gamma)$. The constraint used above is obtained by re-writing the combination of all edge constraints as a combination of elemental contributions, using σ_T to track the sign of the contribution.

B. Elemental Localization

Considering the Lagrangian of the constrained minimization (4),

$$\begin{aligned} \mathcal{L}(\hat{w}; \lambda) \equiv & \frac{1}{2} \int_{\Omega} \nabla \hat{w} \cdot \nabla \hat{w} \, d\Omega - \int_{\Omega} f \hat{w} \, d\Omega \\ & - \sum_{T \in \mathcal{T}_h} \int_{\partial T} \sigma_T \lambda \hat{w} \, d\Gamma, \end{aligned} \quad (6)$$

we recall from the saddle point property of Lagrange multipliers and the strong duality of convex minimizations that for all $\tilde{\lambda} \in \Lambda$

$$\begin{aligned} \varepsilon^- &\leq \inf_{\hat{w} \in \hat{\mathcal{U}}} \mathcal{L}(\hat{w}; \tilde{\lambda}) \\ &\leq \sup_{\lambda \in \Lambda} \inf_{\hat{w} \in \hat{\mathcal{U}}} \mathcal{L}(\hat{w}; \lambda) \\ &= \inf_{\hat{w} \in \hat{\mathcal{U}}} \sup_{\lambda \in \Lambda} \mathcal{L}(\hat{w}; \lambda) = \varepsilon, \end{aligned}$$

where the value at optimality is the minimum total energy of the continuum system, $\varepsilon = \frac{1}{2} \int_{\Omega} \nabla u \cdot \nabla u \, d\Omega - \int_{\Omega} f u \, d\Omega$. The lower bounding minimization for a given $\tilde{\lambda}$ is separable, an important property allowing us to treat each element independently. In order to obtain a lower bound, $\tilde{\lambda}$ cannot be chosen arbitrarily. In the context of finite element approximations, our particular choice for $\tilde{\lambda}$ given below guarantees that the relaxed minimization is bounded from below.

B.1 Approximate Multiplier

We now introduce the finite element approximation of Poisson's equation (1) as means of obtaining an approximate Lagrange multiplier. Once we have solved the finite dimensional Poisson problem: find $u_h \in \mathcal{U}_h$ such that

$$\int_{\Omega} \nabla u_h \cdot \nabla v \, d\Omega = \int_{\Omega} f v \, d\Omega, \quad \forall v \in \mathcal{U}_h, \quad (7)$$

where $\mathcal{U}_h = \{v \in \mathcal{U} \mid v|_T \in \mathbb{P}^p(T), \forall T \in \mathcal{T}_h\}$ for a given polynomial order, p . Once we have obtained u_h , we solve the gradient condition of (6) to obtain λ_h : find $\lambda_h \in \Lambda_h$ such that

$$\begin{aligned} \sum_{T \in \mathcal{T}_h} \int_{\partial T} \sigma_T \lambda_h \hat{v} \, d\Gamma = \\ \int_{\Omega} \nabla u_h \cdot \nabla \hat{v} \, d\Omega - \int_{\Omega} f \hat{v} \, d\Omega, \quad \forall \hat{v} \in \hat{\mathcal{U}}_h, \end{aligned} \quad (8)$$

where $\Lambda_h = \{\lambda \in \Lambda \mid \lambda|_{\gamma} \in \mathbb{P}^p(\gamma), \forall \gamma \in \partial \mathcal{T}_h\}$. We call this the equilibration problem and call any compatible Lagrange multiplier "equilibrating". As mentioned previously, this particular choice for the Lagrange multiplier ensures a finite lower bound.

If a Lagrange multiplier $\lambda_h \in \Lambda_h$ satisfies (8), then $\inf_{\hat{w} \in \hat{\mathcal{U}}} \mathcal{L}(\hat{w}; \lambda_h)$ is bounded from below. To prove this, recall that the null space for the Poisson operator is the one dimensional space of constants, \mathbb{R} , and let $\hat{\mathbb{R}} = \prod_{T \in \mathcal{T}_h} \mathbb{R}$ denote the null space of the broken operator. Considering $\hat{c} \in \hat{\mathbb{R}} \subset \hat{\mathcal{U}}_h$ in the equilibration problem (8) and that any $\hat{w} \in \hat{\mathcal{U}}$ can be represented as $\hat{w}' + \hat{c}$ for $\hat{w}' \in \hat{\mathcal{U}} \setminus \hat{\mathbb{R}}$, it is easily shown that $\mathcal{L}(\hat{w}' + \hat{c}; \lambda_h) = \mathcal{L}(\hat{w}'; \lambda_h)$. For the Poisson equation, equilibration ensures that the null space of the operator does not cause the minimization to become unbounded below. The existence of a minimum now follows from the coercivity of the Poisson operator in \hat{w}' .

While not part of the classical finite element problem set, the equilibration problem has been addressed a number of times and in a number of contexts in the finite element

community, not the least of which is in the context of error estimation. For our implementation, we use a method due to Ladevèze [4], [2] which works well for two-dimensional problems, but note that other methods, such as the flux-splitting method of Ainsworth [2], may be better suited for three-dimensional problems and that some parallel finite element algorithms, such as FETI, solve this problem as part of their domain decomposition strategy [9].

C. Elemental Subproblem

We now write the lower bounding minimization induced by the Lagrange saddle point property as

$$\inf_{\hat{w} \in \hat{\mathcal{U}}} \mathcal{L}(\hat{w}; \lambda_h) = \sum_{T \in \mathcal{T}_h} \inf_{w \in \mathcal{U}(T)} J(w)$$

for

$$\begin{aligned} J(w) \equiv & \frac{1}{2} \int_T \nabla w \cdot \nabla w \, d\Omega - \int_T f w \, d\Omega \\ & - \int_{\partial T} \sigma_T \lambda_h w \, d\Gamma, \end{aligned} \quad (9)$$

and consider a representative minimization subproblem. The minimization subproblem simply corresponds to a Poisson problem with Neumann boundary conditions posed on a single element. We have done nothing to change the nature of original problem, but have only acted to decompose the global problem into a sequence of independent local problems.

We do not require, and in general cannot compute, the exact minimum of the local subproblem, but we do require a lower bound for it and we proceed now to introduce the primary ingredient for obtaining this local lower bound.

If we define the positive functional

$$J^c(\mathbf{q}) \equiv \frac{1}{2} \int_T \mathbf{q} \cdot \mathbf{q} \, d\Omega, \quad (10)$$

where $\mathbf{q} \in \mathcal{H}(\text{div}; T)$ and $\mathcal{H}(\text{div}; T) \equiv \{\mathbf{q} \mid \mathbf{q} \in (L^2(T))^d, \nabla \cdot \mathbf{q} \in L^2(T)\}$ for a problem posed in d spacial dimensions, then we have

$$J(w) \geq -J^c(\mathbf{q}), \quad \forall w \in \mathcal{H}^1(T), \forall \mathbf{q} \in \mathcal{Q}, \quad (11)$$

for the set of functions

$$\mathcal{Q} \equiv \left\{ \mathbf{q} \in \mathcal{H}(\text{div}; T) \mid \begin{aligned} & \nabla \cdot \mathbf{q} = f \text{ in } T \text{ and} \\ & \mathbf{q} \cdot \mathbf{n} = \sigma_T \lambda_h \text{ on } \partial T \end{aligned} \right\}. \quad (12)$$

To prove this, we begin by appealing to the following positive expression

$$0 \leq \frac{1}{2} \int_T (\mathbf{q} - \nabla w)^2 \, d\Omega,$$

for any $w \in \mathcal{H}^1(T)$ and any $\mathbf{q} \in \mathcal{Q}$. This expression expands to

$$0 \leq \frac{1}{2} \int_T \mathbf{q} \cdot \mathbf{q} \, d\Omega + \frac{1}{2} \int_T \nabla w \cdot \nabla w \, d\Omega - \int_T \mathbf{q} \cdot \nabla w \, d\Omega,$$

in which we integrate the last term by parts to obtain

$$0 \leq \frac{1}{2} \int_T \mathbf{q} \cdot \mathbf{q} \, d\Omega + \frac{1}{2} \int_T \nabla w \cdot \nabla w \, d\Omega \\ + \int_T \nabla \cdot \mathbf{q} w \, d\Omega - \int_{\partial T} \mathbf{q} \cdot \mathbf{n} w \, d\Gamma.$$

The pointwise constraints included in the definition of \mathcal{Q} makes this expression equivalent to

$$0 \leq \frac{1}{2} \int_T \mathbf{q} \cdot \mathbf{q} \, d\Omega \\ + \frac{1}{2} \int_T \nabla w \cdot \nabla w \, d\Omega - \int_T f w \, d\Omega \\ - \int_{\partial T} \sigma_T \lambda_h w \, d\Gamma.$$

Identifying $J(w)$ and $J^c(\mathbf{q})$ we arrive at the desired expression for the local lower bound.

To obtain the best possible local lower bound, we might consider the maximization problem

$$\sup_{\mathbf{q} \in \mathcal{Q}} -J^c(\mathbf{q}) \leq \inf_{w \in \mathcal{U}(T)} J(w),$$

from which it is clear that we have derived a classic dual formulation² for our local elemental minimization problem and essentially transformed a primal minimization problem into a dual feasibility problem.

Moreover, we can make these subproblems computable by choosing an appropriate finite set in which to search for \mathbf{q} . At the very least the set must be chosen so that the divergence of its functions contain the forcing function, f , in T and the traces of its functions contain the approximate multiplier, λ_h , on ∂T . Since the finite element method produces polynomial approximations for the continuity multiplier, λ_h , we choose a polynomial approximation for \mathcal{Q} and accept for the moment the limitation this imposes on the forcing, f . In particular, we allow the forcing to be of the same polynomial order as the finite element basis so that the set

$$\mathcal{Q}^q \equiv \mathcal{Q} \cap (\mathbb{P}^q(T))^2, \quad (13)$$

with $p < q$ suffices.

D. Procedure

The complete method for the energy bounds consists of three steps:

1. *Global Approximation:* Find $u_h \in \mathcal{U}_h$ such that

$$\int_{\Omega} \nabla u_h \cdot \nabla v \, d\Omega = \int_{\Omega} f v \, d\Omega, \quad \forall v \in \mathcal{U}_h, \quad (14)$$

and calculate the upper bound $\varepsilon_h^+ = -\frac{1}{2} \int_{\Omega} \nabla u_h \cdot \nabla u_h \, d\Omega$.

2. *Global Equilibration:* Find $\lambda_h \in \Lambda_h$ such that

$$\sum_{T \in \mathcal{T}_h} \int_{\partial T} \sigma_T \lambda_h \hat{v} \, d\Gamma = \\ \int_{\Omega} \nabla u_h \cdot \nabla \hat{v} \, d\Omega - \int_{\Omega} f \hat{v} \, d\Omega, \quad \forall \hat{v} \in \hat{\mathcal{U}}_h. \quad (15)$$

²The classic derivation for the dual of the Poisson problem would begin by letting $\mathbf{q} = \nabla w$ (a statement of Fourier's law in the context of heat conduction) and proceed by eliminating w from the problem.

3. *Energy Bounding Subproblems:* Find ε_T^- such that

$$\varepsilon_T^- = \sup_{\mathbf{q} \in \mathcal{Q}^q} -J^c(\mathbf{q}) \quad (16)$$

for each $T \in \mathcal{T}_h$ and calculate the lower bound $\varepsilon_h^- = \sum_{T \in \mathcal{T}_h} \varepsilon_T^-$.

As previously discussed, the upper bound follows directly from the conforming nature of the finite element approximation and the lower bound follows directly from dual relationship of the local subproblem.

The last step requires the solution of a series of quadratic programming problems with linear equality constraints. Our current implementation reduces the constraints, which have a redundancy resulting from the equilibrium conditions, using the singular value decomposition before solving the constrained maximization problem using the gradient condition. The cost remains low due to the small size of the elemental subproblems.

III. OUTPUT BOUNDS

The lower bounding nature of a dual formulation of Poisson's equation (1) has been understood since at least the 1970's and finite element methods have been formulated directly for the dual problem which have in themselves the lower bounding property, so that the end product of the previous section is not in and of itself particularly novel. What we believe to be novel is our ability to recast non-energy output functionals and, although not presented here, non-symmetric dissipative operators in an analogous framework allowing us to apply the ideas of our particular development of the energy bound to these more general settings.

We will continue to keep the presentation simple by considering only linear functional interior outputs. In particular, we will develop upper and lower bounds, s^\pm , on the output quantity

$$s \equiv \int_{\Omega} f^{\mathcal{O}} u \, d\Omega, \quad (17)$$

where u is the exact solution of Poisson's equation (1).

To begin, we must formulate a generalized analogue to equation (4). There are two parts to this task. First, we must replace the energy with a functional representing the output, which we do by adding to our output an affine scaling of the energy which vanishes at the exact solution. Second, now that the minimization of the objective functional no longer corresponds to the solution of our original equation, we must explicitly ensure its solution by including it as a constraint. Furthermore, to obtain both upper and lower bounds, we consider two cases which vary by the sign of the original output. The resulting pair of con-

strained minimization statements are

$$\begin{aligned} \mp s &= \inf_{\hat{w}^\pm \in \hat{\mathcal{U}}} \mp \int_{\Omega} f^{\mathcal{O}} \hat{w}^\pm \, d\Omega \\ &\quad + \frac{\kappa}{2} \left\{ \int_{\Omega} \nabla \hat{w}^\pm \cdot \nabla \hat{w}^\pm \, d\Omega - \int_{\Omega} f \hat{w}^\pm \, d\Omega \right\} \\ \text{s.t.} \quad &\int_{\Omega} \nabla \hat{w}^\pm \cdot \nabla \psi \, d\Omega = \int_{\Omega} f \psi \, d\Omega, \quad \forall \psi \in \mathcal{U}, \\ &\sum_{T \in \mathcal{T}_h} \int_{\partial T} \sigma_T \lambda \hat{w}^\pm \, d\Gamma = 0, \quad \forall \lambda \in \Lambda, \end{aligned} \quad (18)$$

Paraschivou, Peraire and Patera [7], [8] originally proposed this reformulation in the context of two-level output bounding methods which appeal to a second refined but localized finite element approximation for computing the bounds rather than the dual of the infinite dimensional continuum equations.

Now that we have our starting point, we can proceed more or less mechanically to apply the ideas from the energy bound to this more general context. As you will see, the development is very close to that for the energy bound, but with the extra burden of carrying an additional Lagrange multiplier for the equilibrium constraint and of managing the concurrent development of both upper and lower bounds on the output, as neither arise implicitly from the finite element discretization.

A. Localization

Considering the Lagrangian of the above minimization (18),

$$\begin{aligned} \mathcal{L}^\pm(\hat{w}^\pm; \psi^\pm, \lambda^\pm) &\equiv \\ &\mp \int_{\Omega} f^{\mathcal{O}} \hat{w}^\pm \, d\Omega \\ &\quad + \frac{\kappa}{2} \left\{ \int_{\Omega} \nabla \hat{w}^\pm \cdot \nabla \hat{w}^\pm \, d\Omega - \int_{\Omega} f \hat{w}^\pm \, d\Omega \right\} \\ &\quad + \int_{\Omega} f \psi^\pm \, d\Omega - \int_{\Omega} \nabla \hat{w}^\pm \cdot \nabla \psi^\pm \, d\Omega \\ &\quad - \sum_{T \in \mathcal{T}_h} \int_{\partial T} \sigma_T \lambda^\pm \hat{w}^\pm \, d\Gamma, \end{aligned} \quad (30)$$

we know, as we did for the energy bound, from the saddle point property of Lagrange multipliers and from the strong duality of convex minimizations that for all $(\tilde{\psi}^\pm, \tilde{\lambda}^\pm) \in \mathcal{U} \times \Lambda$

$$\begin{aligned} \mp s^\pm &\leq \inf_{\hat{w}^\pm \in \hat{\mathcal{U}}} \mathcal{L}^\pm(\hat{w}^\pm; \tilde{\psi}^\pm, \tilde{\lambda}^\pm) \\ &\leq \sup_{\psi^\pm \in \mathcal{U}} \inf_{\hat{w}^\pm \in \hat{\mathcal{U}}} \mathcal{L}^\pm(\hat{w}^\pm; \psi^\pm, \lambda^\pm) \\ &= \inf_{\hat{w}^\pm \in \hat{\mathcal{U}}} \sup_{\psi^\pm \in \mathcal{U}} \mathcal{L}^\pm(\hat{w}^\pm; \psi^\pm, \lambda^\pm) = \mp s, \end{aligned}$$

We proceed, as we did for the energy bound, to obtain approximate Lagrange multipliers with a finite element discretization of the gradient condition of the Lagrangian (30) and the definitions $\psi_h^\pm = \pm \psi_h$ and $\lambda_h^\pm = \frac{\kappa}{2} \lambda_h^u \pm \lambda_h^\psi$.

The procedure is summarized in Figure 1. In the sections below we derive the dual relationship and elemental subproblems for the output bounds procedure.

B. Local Output Dual

Restricting our attention to a single elemental subproblem, $T \in \mathcal{T}_h$, we first re-write our local Lagrangian functional in a form suitable for applying the ideas developed for the energy bound. Every term other than the dissipative energy term, $\frac{\kappa}{2} \int_T \nabla w \cdot \nabla w \, d\Omega$, must be in Galerkin-weak form, which we can do in the present case by application of the Green's identity $-\int_T \nabla u \cdot \nabla w \, d\Omega = \int_T w \Delta u \, d\Omega - \int_{\partial T} w (\nabla u \cdot \mathbf{n}) \, d\Gamma$ to obtain

$$\begin{aligned} \mathcal{L}_T^\pm(w^\pm; \pm \psi_h, \frac{\kappa}{2} \lambda_h^u \pm \lambda_h^\psi) &\equiv \\ &\frac{\kappa}{2} \left\{ \int_T \nabla w^\pm \cdot \nabla w^\pm \, d\Omega - \int_T f w^\pm \, d\Omega \right. \\ &\quad \left. - \int_{\partial T} \sigma_T \lambda_h^u w^\pm \, d\Gamma \right\} \\ &\pm \left\{ - \int_T (f^{\mathcal{O}} - \Delta \psi_h) w^\pm \, d\Omega \right. \\ &\quad \left. - \int_{\partial T} (\nabla \psi_h \cdot \mathbf{n} + \lambda_h^\psi) w^\pm \, d\Gamma \right. \\ &\quad \left. + \int_T f \psi_h \, d\Omega \right\}. \end{aligned} \quad (31)$$

The functional we wish to minimize over w^\pm can now be defined as

$$\begin{aligned} J^\pm(w^\pm) &\equiv \frac{\kappa}{2} \int_T \nabla w^\pm \cdot \nabla w^\pm \, d\Omega \\ &\quad - \int_T f^\pm w^\pm \, d\Omega \\ &\quad - \int_{\partial T} g^\pm w^\pm \, d\Gamma, \end{aligned} \quad (32)$$

for $f^\pm \equiv \frac{\kappa}{2} f \pm \{f^{\mathcal{O}} - \Delta \psi_h\}$ and $g^\pm \equiv \frac{\kappa}{2} \sigma_T \lambda_h^u \pm \{\sigma_T \lambda_h^\psi + \nabla \psi_h \cdot \mathbf{n}\}$.

The local dual problem can be derived as it was for the energy bound, but with modified data and the addition of the tuning parameter, κ ,

$$0 \leq \frac{1}{2\kappa} \int_T (\mathbf{q}^\pm - \kappa \nabla w)^2 \, d\Omega, \quad (33)$$

from which, after defining the sets \mathcal{Q}^\pm for the output subproblems as

$$\begin{aligned} \mathcal{Q}^\pm &\equiv \{ \mathbf{q} \in \mathcal{H}(\text{div}; T) \mid \nabla \cdot \mathbf{q} = -f^\pm \text{ in } T \text{ and} \\ &\quad \mathbf{q} \cdot \mathbf{n} = g^\pm \text{ on } \partial T \} \end{aligned} \quad (34)$$

and defining the complementary energy functional as

$$J^c(\mathbf{q}^\pm) \equiv \frac{1}{2\kappa} \int_T \mathbf{q}^\pm \cdot \mathbf{q}^\pm \, d\Omega, \quad (35)$$

we arrive at our local dual relationship

$$J^\pm(w^\pm) \geq -J^c(\mathbf{q}^\pm), \quad \forall w^\pm \in \mathcal{H}^1(T), \forall \mathbf{q}^\pm \in \mathcal{Q}^\pm, \quad (36)$$

1. *Global Finite Element Approximation:*Find $u_h \in \mathcal{U}_h$ such that

$$\int_{\Omega} \nabla u_h \cdot \nabla v \, d\Omega = - \int_{\Omega} f v \, d\Omega, \quad \forall v \in \mathcal{U}_h, \quad (19)$$

Find $\psi_h \in \mathcal{U}_h$ such that

$$\int_{\Omega} \nabla v \cdot \nabla \psi_h \, d\Omega = - \int_{\Omega} f^{\mathcal{O}} v \, d\Omega, \quad \forall v \in \mathcal{U}_h, \quad (20)$$

2. *Global Finite Element Equilibration:*Find $\lambda_h^u \in \Lambda_h$ such that

$$\sum_{T \in \mathcal{T}_h} \int_{\partial T} \sigma_T \lambda_h^u \hat{v} \, d\Gamma = \int_{\Omega} \nabla u_h \cdot \nabla \hat{v} \, d\Omega - \int_{\Omega} f \hat{v} \, d\Omega, \quad \forall \hat{v} \in \hat{\mathcal{U}}_h, \quad (21)$$

Find $\lambda_h^\psi \in \Lambda_h$ such that

$$\sum_{T \in \mathcal{T}_h} \int_{\partial T} \sigma_T \lambda_h^\psi \hat{v} \, d\Gamma = - \int_{\Omega} f \hat{v} \, d\Omega - \int_{\Omega} \nabla \hat{v} \cdot \nabla \psi_h \, d\Omega, \quad \forall \hat{v} \in \hat{\mathcal{U}}_h, \quad (22)$$

3. *Output Bounding Subproblems:*Find $\mathbf{q}^u \in \mathcal{Q}^{u,q}$ such that

$$\mathbf{q}^u = \arg \inf_{\mathbf{q} \in \mathcal{Q}^{u,q}} J^c(\mathbf{q}), \quad (23)$$

find $\mathbf{q}^\psi \in \mathcal{Q}^{\psi,q}$ such that

$$\mathbf{q}^\psi = \arg \inf_{\mathbf{q} \in \mathcal{Q}^{\psi,q}} J^c(\mathbf{q}), \quad (24)$$

and compute

$$\bar{s}_T = \sum_{T \in \mathcal{T}_h} \int_T \mathbf{q}^u \cdot \mathbf{q}^\psi \, d\Omega - \int_T f \psi_h \, d\Omega, \quad (25)$$

$$z_T^u = \frac{1}{2} \int_T \mathbf{q}^u \cdot \mathbf{q}^u \, d\Omega, \quad (26)$$

$$z_T^\psi = \frac{1}{2} \int_T \mathbf{q}^\psi \cdot \mathbf{q}^\psi \, d\Omega, \quad (27)$$

for each $T \in \mathcal{T}_h$.4. *Calculate Output Bounds:*

Calculate

$$s_h^\pm = \bar{s}_h \pm 2\sqrt{z_h^u z_h^\psi}. \quad (28)$$

for

$$\bar{s}_h = \sum_{T \in \mathcal{T}_h} \bar{s}_T, \quad z_h^u = \sum_{T \in \mathcal{T}_h} z_T^u, \quad z_h^\psi = \sum_{T \in \mathcal{T}_h} z_T^\psi. \quad (29)$$

Fig. 1. The Output Bound Procedure

and our local output bounding subproblems

$$s_T^\pm = - \int_T f \psi_h \, d\Omega \pm \inf_{\mathbf{q}^\pm \in \mathcal{Q}^\pm} J^c(\mathbf{q}^\pm). \quad (37)$$

basis, there are no difficulties in continuing to choose our dual approximation space as

$$\mathcal{Q}^{\pm,q} \equiv \mathcal{Q}^\pm \cap (\mathbb{P}^q(T))^2, \quad (38)$$

As the terms in the data of the dual feasibility constraints are the just polynomial functions in the local finite element

with $p < q$ still sufficing. The subproblems are solved in the same manner as for the energy bounds.

B.1 Optimal Tuning

The introduction of the tuning parameter, κ , allows us to maximize the sharpness of the computed bounds. Consider for a single elemental subproblem the definition $\mathbf{q} = \kappa \mathbf{q}^u \pm \mathbf{q}^\psi$. Propagation of this definition into the elemental subproblem reveals through the linearity of the gradient condition that indeed \mathbf{q}^u and \mathbf{q}^ψ can be computed independently. The independent problems become

$$\begin{aligned} \mathbf{q}^u &= \arg \inf_{\mathbf{q} \in \mathcal{Q}^{u,q}} J^c(\mathbf{q}), \\ \mathbf{q}^\psi &= \arg \inf_{\mathbf{q} \in \mathcal{Q}^{\psi,q}} J^c(\mathbf{q}), \end{aligned} \quad (39)$$

for

$$\begin{aligned} \mathcal{Q}^u &\equiv \{ \mathbf{q} \in \mathcal{H}(\text{div}; T) \mid \nabla \cdot \mathbf{q} = f \text{ in } T \text{ and} \\ &\quad \mathbf{q} \cdot \mathbf{n} = \sigma_T \lambda_h^u \text{ on } \partial T \}, \\ \mathcal{Q}^\psi &\equiv \{ \mathbf{q} \in \mathcal{H}(\text{div}; T) \mid \nabla \cdot \mathbf{q} = f^\mathcal{O} - \Delta \psi_h \text{ in } T \text{ and} \\ &\quad \mathbf{q} \cdot \mathbf{n} = \sigma_T \lambda_h^\psi + \nabla \psi_h \cdot \mathbf{n} \text{ on } \partial T \}, \end{aligned} \quad (40)$$

as well as $\mathcal{Q}^{u,q} \equiv \mathcal{Q}^u \cap (\mathbb{P}^q(T))^2$ and $\mathcal{Q}^{\psi,q} \equiv \mathcal{Q}^\psi \cap (\mathbb{P}^q(T))^2$.

Let $z_T^u = \frac{1}{2} \int_T \mathbf{q}^u \cdot \mathbf{q}^u \, d\Omega$, $z_T^\psi = \frac{1}{2} \int_T \mathbf{q}^\psi \cdot \mathbf{q}^\psi \, d\Omega$, then

$$s_h^\pm = \bar{s}_h \pm \kappa z^u \pm \frac{1}{\kappa} z^\psi,$$

where $\bar{s}_h = \sum_{T \in \mathcal{T}_h} \int_T \mathbf{q}^u \cdot \mathbf{q}^\psi \, d\Omega - \int_T f \psi_h \, d\Omega$ and $z = \sum_{T \in \mathcal{T}_h} z_T$.

Maximizing the lower bound and minimizing the upper bound with respect to κ yields

$$\kappa^2 = \frac{z^\psi}{z^u}, \quad (41)$$

with which the output bounds can be written as

$$s_h^\pm = \bar{s}_h \pm 2\sqrt{z^u z^\psi}. \quad (42)$$

IV. NUMERICAL RESULTS

We verify the method numerically for three cases: constant forcing on the unit square, linear forcing on the unit square, and unforced L-shaped domain with a corner singularity. Linear finite elements, $p = 1$, and quadratic subproblems, $q = 2$, are employed with domain average output for all cases.

All three cases have analytically exact solutions with which we are able to verify the method and calculate the effectivities of the bounds,

$$\theta^\pm = \frac{|s - s_h^\pm|}{|s - s_h|}, \quad (43)$$

which indicate the sharpness by comparing the error in the bounds to the error in the finite element approximation. The results are summarized in Table I and Figure 2.

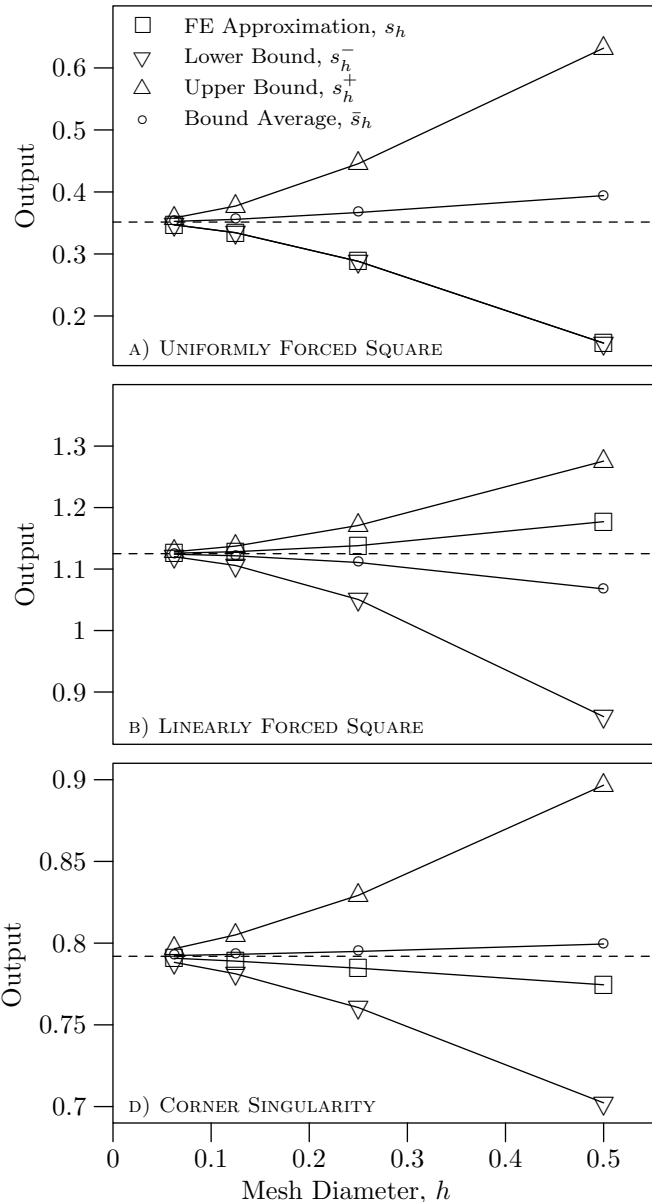


Fig. 2. Plotted output bounds with finite element approximations for the three numerical test cases. The exact output is indicated by a dashed line.

A. Uniformly Forced Square Domain

The first case is a uniformly forced unit square domain. The analytical solution is given by

$$u(x, y) = \left(\frac{8}{\pi}\right)^2 \sum_{\text{odd } i=1}^{\infty} a_{ij} \cos\left(i\frac{\pi}{2}x\right) \cos\left(j\frac{\pi}{2}y\right),$$

with

$$a_{ij} = \frac{(-1)^{(i+j)/2-1}}{ij(i^2 + j^2)}.$$

This case is special in that the forcing and output are identical and the boundary data is homogeneous, leading to primal and adjoint problem data which differ by only a

h	Uniformly Forced Square				Linearly Forced Square				Corner Singularity			
	s_-	s^+	θ^-	θ^+	s_-	s^+	θ^-	θ^+	s_-	s^+	θ^-	θ^+
$\frac{1}{2}$	0.156	0.632	1.0	1.40	0.860	1.276	5.1	2.9	0.702	0.897	5.1	6.0
$\frac{1}{4}$	0.288	0.446	1.0	1.48	1.050	1.171	5.7	3.5	0.761	0.829	4.3	5.1
$\frac{1}{8}$	0.334	0.377	1.0	1.50	1.106	1.137	5.9	3.8	0.781	0.805	3.6	4.4
$\frac{1}{16}$	0.347	0.358	1.0	1.51	1.120	1.128	6.0	3.8	0.788	0.797	3.1	3.9

TABLE I

TABULATED OUTPUT BOUNDS AND EFFECTIVITIES FOR THE THREE NUMERICAL TESTS CASES.

sign. It is well known that for this special case, called compliance, the finite element approximation for the output is a lower bound. The numerical results demonstrate that our method, while more expensive, does no worse than the inherent bound for this special case. The results for both the finite element approximation and the output bounds asymptotically approach the optimal finite element convergence rate of $O(h^2)$. This example also evince that the bound average, \bar{s}_h , can sometimes be a more accurate output approximation than the that from the finite element approximation.

B. Linearly Forced Square Domain

The second case is a linearly forced square domain with the forcing and non-homogeneous boundary conditions chosen to produce the exact solution

$$u(x, y) = \frac{3}{2}y^2(1 - y) + 4xy.$$

As this test case is not a special case, the convergence histories of Figure 2b depict the more general situation in which none of the computed quantities coincide. Whereas in the first example we saw that the bound average can possibly be a more accurate output approximation than the finite element approximation, in this example we see that this definitely not always true since the finite element approximation for the output is 0.5% better. As for the first example, the results for both the finite element approximation and the output bounds asymptotically approach the optimal finite element convergence rate of $O(h^2)$.

C. Unforced Corner Domain

Last, we consider the Laplace equation on a non-convex domain. The domain is the standard L-shaped domain with a reentrant corner. The boundary conditions were chosen to produce the exact solution

$$u(r, \phi) = r^{\frac{2}{3}} \sin \frac{2}{3}\phi,$$

where r is the distance from the corner point and ϕ is the angle from the upper surface of the corner.

In this example we demonstrate that the bounds are valid even for problems with singularities. The results for both the finite element approximation and the output bounds asymptotically approach the optimal finite element convergence rate of $O(h^{4/3})$ for elliptic problems posed on a

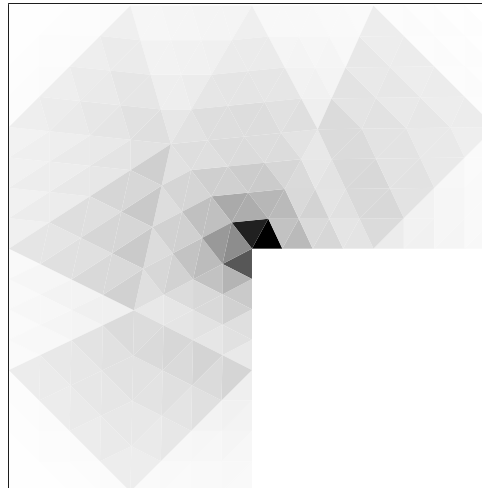
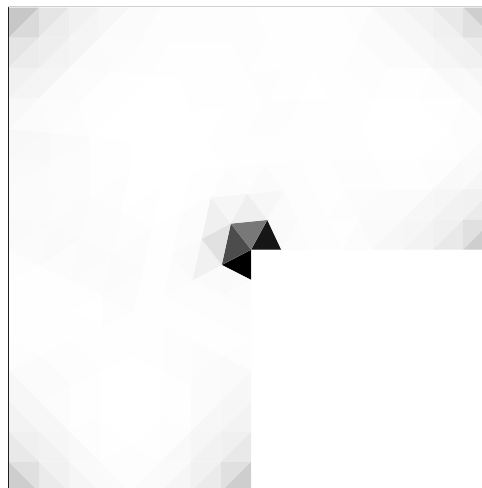
A) DISTRIBUTION OF z_T^u .B) DISTRIBUTION OF z_T^ψ .

Fig. 3. Distributions of principle bound gap components in unforced corner domain numerical test case. Darker triangles imply larger contributions to the bound gap.

domain with right-angled reentrant corner. Once again we see that the bound average has the potential to be a better output approximation than the finite element method.

Figure 3 shows the distribution of the elemental bound quantities, z_T^u and z_T^ψ , which contribute to the global bound gap. The distributions show that elements closer to the singularity contribute more to the bound gap. Thus, an adaptive scheme which equilibrated these contributions would preferentially refine the mesh near the singularity.

REFERENCES

- [1] Pedro Morin, Ricardo H. Nochetto, and Kunibert G. Siebert, "Convergence of adaptive finite element methods," *SIAM Review*, vol. 44, no. 4, pp. 631–658, 2002.
- [2] Mark Ainsworth and J. Tinsley Oden, "A posteriori error estimation in finite element analysis," *Computer Methods in Applied Mechanics and Engineering*, , no. 142, pp. 1–88, March 1997.
- [3] B.M. Fraeijs de Veubeke, "Displacement and equilibrium models in the finite element method," in *B.M. Fraeijs de Veubeke Memorial Volume of Selected Papers*, Michel geradin, Ed. Sijthoff and Noordhoff International Publishers, 1980.
- [4] Pierre Ladevèze and D. Leguillon, "Error estimate procedure in the finite element method and applications," *SIAM Journal of Numerical Analysis*, vol. 20, no. 3, pp. 485–509, June 1983.
- [5] D.W. Kelly, "The self-equilibration of residuals and complementary a posteriori error estimates in the finite element method," *International Journal for Numerical Methods in Engineering*, vol. 20, pp. 1491–1506, 1984.
- [6] Philippe Destuynder and Brigitte Métivet, "Explicit error bounds in a conforming finite element method," *Mathematics of Computation*, vol. 68, no. 228, pp. 1379–1396, 1999.
- [7] Marius Paraschivoiu, Jaime Peraire, and Anthony T. Patera, "A posteriori finite element bounds for linear-functional outputs of elliptic partial differential equations," *Computer Methods in Applied Mechanics and Engineering*, vol. 150, no. 1-4, pp. 289–312, December 1997.
- [8] Marius Paraschivoiu and Anthony T. Patera, "A hierarchical duality approach to bounds for the outputs of partial differential equations," *Computer Methods in Applied Mechanics and Engineering*, vol. 158, no. 3-4, pp. 389–407, June 1998.
- [9] Marius Paraschivoiu, "A posteriori finite element output bounds in three space dimensions using the feti method," *Computer Methods in Applied Mechanics and Engineering*, vol. 190, pp. 6629–6640, 2001.